JACS
JOURNAL OF THE AMERICAN CHEMICAL SOCIETY

ARTICLE

pubs.acs.org/JACS

Rhodium Phosphine−π-Arene Intermediates in the Hydroamination of Alkenes

Zhijian Liu, Hideaki Yamamichi, Sherzod T. Madrahimov, and John F. Hartwig*

Department of Chemistry, University of Illinois, 600 South Mathews Avenue, Urbana, Illinois 61801-3602, United States

Supporting Information

ABSTRACT: A detailed mechanistic study of the intramolecular hydroamination of alkenes with amines catalyzed by rhodium complexes of a biaryldialkylphosphine is reported. The active catalyst is shown to contain the phosphine ligand bound in a κ^1, η^6 form in which the arene is π-bound to rhodium. Addition of deuterated amine to an internal olefin showed that the reaction occurs by trans addition of the N−H bond across the C=C bond, and this stereochemistry implies that the reaction occurs by nucleophilic attack of the amine on a coordinated alkene. Indeed, the cationic rhodium fragment binds the alkene over the secondary amine, and the olefin complex was shown to be the catalyst resting state. The reaction was zero-order in substrate, when the concentration of olefin was high, and a primary isotope effect was observed. The primary isotope effect, in combination with the observation of the alkene complex as the resting state, implies that nucleophilic attack of the amine on the alkene is reversible and is followed by turnover-limiting protonation. This mechanism constitutes an unusual pathway for rhodium-catalyzed additions to alkenes and is more closely related to the mechanism for palladium-catalyzed addition of amide N−H bonds to alkenes.

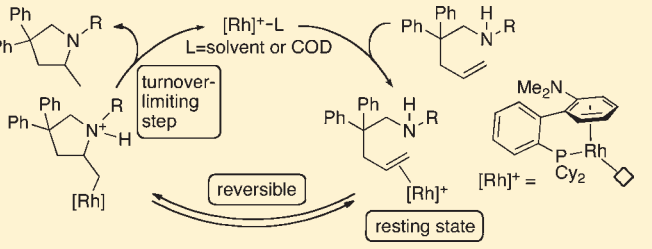

INTRODUCTION

The hydroamination of alkenes has been studied for decades, but only recently have complexes containing late transition metals been identified that catalyze the additions of amines to unactivated olefins.[1−4] After catalysts for the addition of aniline to strained alkenes[5,6] and acrylamide[7,8] were identified, palladium complexes that catalyze the additions of amines to unstrained vinylarenes,[9,10] and complexes containing rhodium that add amines to vinylarenes with the opposite regioselectivity[11] in high yields[12] were discovered. Complexes of platinum were then shown to catalyze the intramolecular additions of amines to alkenes,[13] and a simple iridium system has been shown to cyclize aminoalkenes when they are conformationally biased for intramolecular reactions.[14,15] In parallel, a series of systems that catalyze the intramolecular additions of amides and carbamates to alkenes were uncovered.[16−26]

We recently reported the discovery of two rhodium catalysts that are particularly active for the additions of alkylamines to alkenes[27,28] and a recent study built upon the first of these systems to develop enantioselective versions of this reaction.[29] One of the catalysts we reported was based on the combination of $[Rh(COD)_2]BF_4$ and a biaryldialkylphosphine (**L**) first developed for palladium-catalyzed cross coupling.[27] This combination of metal and ligand was unique for late-metal systems and remains a rare system because it catalyzes the cyclization of aminoalkenes lacking substituents on the chain linking the two functional groups that favor cyclization. This combination also catalyzed the addition of amines to internal alkenes and catalyzed additions of both primary and secondary amines to alkenes.[30] The second catalyst we reported contained an aminophosphine analog of Xantphos and was particularly active for cyclization of primary aminoalkenes.[28]

Although these studies revealed an unusually broad scope for alkene hydroamination, the structure of the complex responsible for the reactivity of the catalyst containing the biaryldialkylphosphine and the basic steps of the reaction were not identified. Several types of mechanisms have been shown to lead to hydroamination processes catalyzed by late transition metals. One of these mechanisms includes oxidative addition of an N−H bond, migratory insertion of the alkene into the metal−nitrogen bond, and reductive elimination to form a C−H bond.[5] A second mechanism, more commonly followed by lanthanide[3,31,32] and group IV metals,[32−36] involves migratory insertion of the alkene into the metal-amide, followed by proton transfer.[37] A third mechanism is thought to occur by nucleophilic attack of an amine on a coordinated alkene, followed by proton transfer to release the amine product.[13,38] Finally, reactions of amines with alkynes catalyzed by some group IV complexes have been shown to occur by [2 + 2] additions of alkenes to metal−imido intermediates,[39,40] and reactions of some aminoalkenes catalyzed by zirconium(IV) complexes have been proposed to occur by an analogous mechanism.[41,42]

Rhodium catalysts are well-known to add H−X bonds to alkenes by a pathway involving oxidative addition, migratory insertion, and reductive elimination.[43] Hydrogen, syngas,

Received: July 6, 2010
Published: February 10, 2011

dx.doi.org/10.1021/ja1057949 | J. Am. Chem. Soc. 2011, 133, 2772–2782

silanes, boranes, and stannanes all react with alkenes by such a pathway, and, therefore, these additions occur in a syn fashion across the alkene.[43−45] In the absence of mechanistic information on the rhodium system that we identified, it was unclear if the hydroamination process would occur by a mechanism akin to the addition of these other reagents, or if the hydroamination would occur by a pathway more akin to the addition of N−H bonds by other catalysts.

Mechanistic studies have implied that palladium-catalyzed additions of the N−H bonds of amides and carbamates to alkenes[26] and platinum-catalyzed additions of secondary amines to alkenes[13] occur by nucleophilic attack on an alkene, followed by proton transfer. Analogous steps have been shown to occur during the addition of amines and carbamates to allenes catalyzed by complexes of gold.[46,47]

Such a path involving nucleophilic attack on a coordinated alkene would be unusual for a complex of rhodium for several reasons. First, nucleophilic attack on an alkene bound to rhodium is not a common reaction.[48,49] Second, the only prior mechanistic information on alkene amination catalyzed by rhodium, oxidative aminations of vinylarenes with dialkylamines catalyzed by $[Rh(COD)_2]BF_4$ and PPh_3, led to ambiguous conclusions about whether the process occurred by nucleophilic attack on a coordinated vinylarenes or oxidative addition of the amine, insertion of the olefin, and β-hydrogen elimination.[11] Although work from the authors' group on a different rhodium-catalyzed process implied that nucleophilic attack on a vinylarene occurred as the first step, nucleophilic attack on an alkene complex is different; the stable η^3-benzyl-type complex formed by attack on a coordinated vinylarene[12] is not formed from attack on a coordinated alkene.

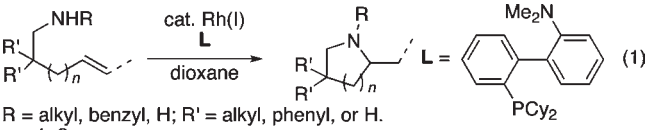

R = alkyl, benzyl, H; R' = alkyl, phenyl, or H.
n = 1, 2.

To begin to reveal the factors controlling the activity of this catalyst and the selectivity for products from hydroamination vs olefin isomerization and oxidative amination,[12] we have conducted mechanistic studies of the process in eq 1. We report the structure of the active form of the rhodium catalyst, the relative binding affinity of this species toward alkenes and secondary amines, the resting state of the catalyst, the turnover-limiting step of the catalytic cycle, and the stereochemistry of the addition process. These data support a mechanism involving trans addition and allow us to propose an experimentally supported hypothesis to explain the selectivity for formation of products from hydroamination over oxidative amination.

RESULTS AND DISCUSSION

1. Identification of the Metal−Ligand Core of the Active Catalyst. The catalyst we initially reported was generated from the biaryldialkylphosphine (**L**) in eq 2[50] and $[Rh(COD)_2]BF_4$, but the structure of the species in the catalytic system was unknown. Mixing these two materials (in the dioxane solvent of the initial catalytic system) led to only a small amount of product from binding of **L**. To favor coordination of the ligand, we studied the reaction of the phosphine with the species formed from $[Rh(ethylene)_2Cl]_2$ and $AgBF_4$. To ensure solubility, we conducted the reaction of this species, as generated in THF, with

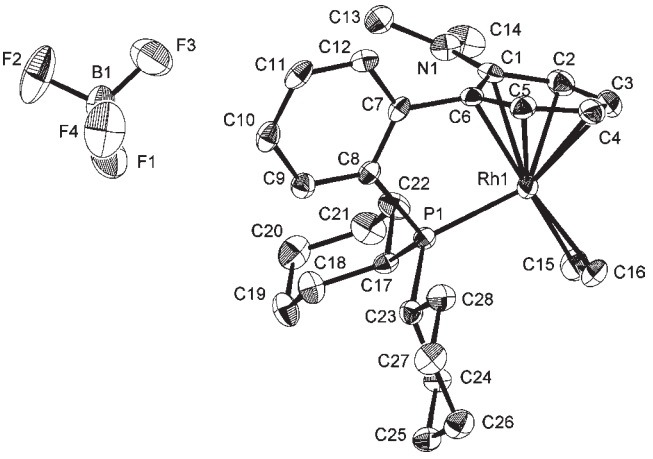

Figure 1. ORTEP diagram of $[Rh(L)(C_2H_4)]BF_4$ (**1**). Ellipsoids are shown at 50% probability. All hydrogen atoms are omitted for clarity.

the phosphine in CH_2Cl_2. This reaction is depicted in eq 2 and formed a single complex **1**, which contained one coordinated alkene and one **L**. NMR spectroscopy and X-ray diffraction showed that the ligand **L** was bound in the tethered η^6, κ^1 mode shown in this equation. A series of complexes of Cp and arene ligands tethered to phosphorus donors have been prepared, but few contain just a two-carbon linker. Such a binding mode was observed previously by Faller et al. between ruthenium and this biaryldialkylphosphine when studying complexes for reactions catalyzed by Lewis acids[51] and by Werner et al. with a rhodium complex of a ligand containing an aliphatic bridge between the arene and the phosphine.[52]

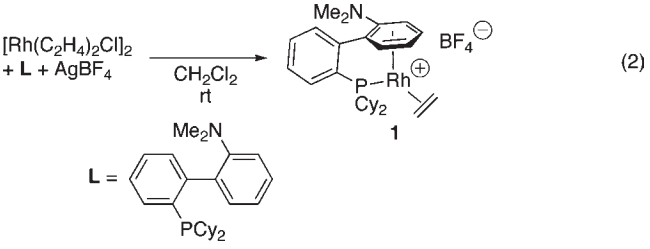

An ORTEP diagram of **1** is shown in Figure 1. This structure clearly contains the biaryldialkylphosphine bound in an η^6, κ^1 mode. The dimethylamino group is nearly coplanar with the arene ring, and the nitrogen is almost perfectly planar ($\sum_{CNC} = 359.8°$), suggesting that the dimethylamino group serves as a strong electron donor to the coordinated arene ring. The arene ring is not strictly planar. The C6 carbon atom lies out of the arene plane by 0.11 Å, and the angle consisting of the centroid of the arene and the two carbon atoms of the C−C bond between the coordinated and bridging arene rings is 170.6°. Thus, the arene−phosphine chelate contains observable strain. The Rh−P distance (2.2383(8) Å) is 0.06 Å shorter than the average Rh−P distance involving phosphine ligands for the compounds in the CCD and similar to the 2.251(2) Å Rh−P distance in a closely related rhodium complex containing an η^6, κ^1-arene−phosphine ligand linked by a three-carbon aliphatic tether.[52]

Finally, the metric parameters of the bound ethylene are only slightly distorted from those of free ethylene and close to those of classic Pd(II) or Pt(II) species. The C−C distance of 1.380(6) Å in **1** is similar to the 1.37 Å distance in Zeise' salt,[53] shorter than the

dx.doi.org/10.1021/ja1057949 |J. Am. Chem. Soc. 2011, 133, 2772–2782

Scheme 1

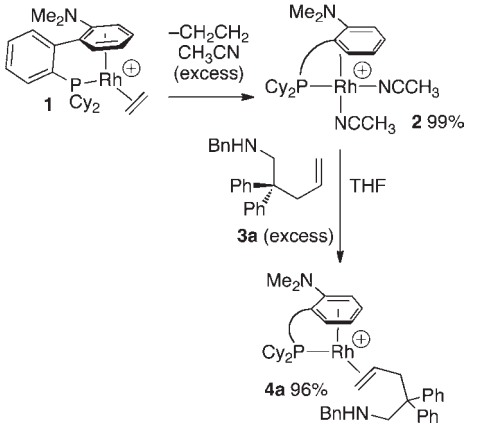

1.43 Å distance in $[Pt(PPh_3)_2(C_2H_4)]$,[54] similar to the 1.38 and 1.39 Å distances in $[Pd(COD)Cl_2]$,[55] similar to the 1.35 Å distance in a cationic Pd−ethylene complex containing a P,O ligand,[56] slightly shorter than the 1.40(3) Å distance in the related Rh−ethylene complex,[52] and slightly longer than the 1.31−1.34 Å distance in a typical free alkene.[57] The Rh−C distances (2.134(3) Å for both) are similar to those of known rhodium−ethylene complexes (2.10(4), 2.15(4), 2.162(17), and 2.172(17) Å for a related half-sandwich-Rh-ethylene complex).[52] These data indicate that the structure of the complex is more akin to olefin complexes, such as Zeise' salt, that react with nucleophiles than to electron-rich complexes, such as $Pt(PPh_3)_2(C_2H_4)$, that react with electrophiles.

Solution NMR spectra indicate that the η^6, κ^1 mode is also adopted by the complex in solution. In particular, the ^{1}H NMR signals for the amino-substituted arene are observed between 5.42 and 6.68 ppm. The ^{13}C NMR signals for the same arene are observed between 89.6 and 141.4 ppm and contain coupling to rhodium.

2. Coordination Chemistry of the Active Catalyst. 2.1. Synthesis and Structures of Rhodium Aminoalkene Complexes. Rhodium complexes of the secondary and primary aminoalkenes were generated indirectly from ethylene complex **1**. The ethylene in complex **1** was not displaced by the secondary aminoalkene in a closed system, but the complex of this substrate was generated by the method shown in Scheme 1. Dissolution of the ethylene complex in acetonitrile released ethylene from the system and formed the acetonitrile complex **2**. Although we could not determine the number of coordinated acetonitriles in complex **2** because it is stable only in acetonitrile, we were able to gather data on the solid-state structure by X-ray diffraction. An ORTEP diagram for this compound is shown in Figure 2.

This compound crystallized with two molecules in the asymmetric unit. The biaryldialkylphosphine is bound in an η^2, κ^1 mode, rather than the η^6, κ^1 mode of the ethylene complex **1**. The Rh−C_{ipso} distance (2.219(3) and 2.216(3) Å) in the η^2-arene is roughly 0.05 Å longer than that in the η^6-arene of **1** (2.166(3) Å), and the Rh−C_{ortho} distance (2.214(3) and 2.215(3) Å) in **2** is 0.06 Å shorter than that in **1** (2.271(3) Å). The dimethylamino group on the arene is more pyramidized ($\sum_{CNC}$ = 352.6 and 356.7°) than that in the ethylene complex **1** ($\sum_{CNC}$ = 359.8°). Despite the change in hapticity of the arene, the Rh−P distance (2.2058(9) and 2.2147(9) Å) is only 0.02 Å shorter than that in complex **1** (2.2383(8) Å). Finally, the Rh−N distance (2.104(3) and

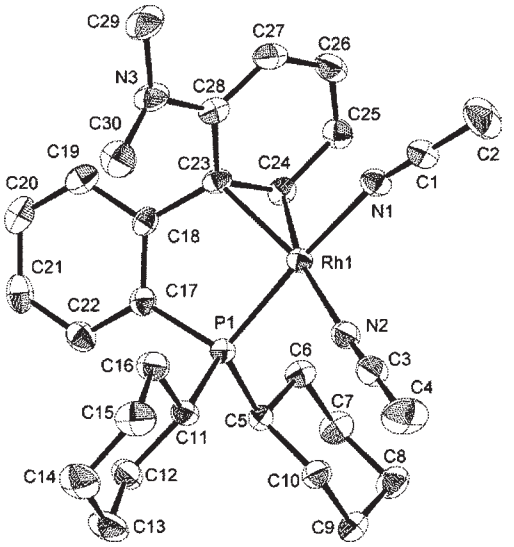

Figure 2. ORTEP diagram of the cationic portion of $[Rh(L)(NCMe)_2]BF_4$ (**2**). Ellipsoids are shown at 50% probability. All hydrogen atoms are omitted for clarity.

2.096(3) Å) for the nitrile trans to the phosphine is longer than the Rh−N distance (2.028(3) and 2.022(3) Å) for the nitrile located trans to the η^2-arene ligand, implying that the phosphine has a larger trans influence than the η^2-coordinated π system of the arene. The ^{1}H NMR signal for the hydrogen on the bound ortho carbon was observed at 5.42 ppm, and the ^{13}C NMR signals for the two bound carbons were observed at 88.5 and 89.1 ppm with larger J_{Rh-C} values (9 and 12 Hz, respectively) than those in complex **1** (2−3 Hz).

Treatment of this acetonitrile complex with the secondary aminoalkene **3a** led to coordination of the olefinic portion of **3a**, not the amino group, to form complex **4a** as a 1.6:1 ratio of two diastereomers. This binding mode of the reactant was clearly revealed by upfield signals of the bound alkene at 2.54−3.05 ppm in the ^{1}H NMR spectrum and upfield signals at 43−46 and 63−66 ppm with nearly equivalent J_{Rh-C} values (13 and 11 Hz, respectively) in the ^{13}C NMR spectrum of **4a**. This binding of an alkene over an amine is unusual for a cationic complex.[49] The η^6 binding mode of the arene is evidenced by the signals for the coordinated ring in the ^{1}H NMR spectrum upfield of the aromatic region and signals for the bound C−H in the $^{13}C\{^1H\}$ NMR spectrum between 90 and 110 ppm.

Because the combination of $[Rh(COD)_2]BF_4$ and **L** also catalyzes the cyclization of primary aminoalkenes and this class of substrate generally has been less reactive toward late-metal catalysts for hydroamination, we tested the binding of primary amine **3b** to ethylene complex **1** by addition of the aminoalkene to the ethylene complex, as shown in Scheme 2. In this case, addition of the primary aminoalkene **3a** occurred without the need to generate the nitrile complex as an intermediate. Direct reaction of **1-SbF$_6$** with **3b** formed **4b** in high yield.

The structure of the primary aminoalkene complex **4b** was much different from that of the secondary aminoalkene complex **4a**. Both the amine and the alkene portions of the primary aminoalkene bind to rhodium in **4b**, and two diastereomers of the adduct are observed. The ratio of diastereomers was ca. 3:1 in methylene chloride, but over 10:1 in dioxane. These two diastereomers result from different relative configurations created by binding to the two faces of the arene and the alkene. The ratios of these diastereomers

dx.doi.org/10.1021/ja1057949 |J. Am. Chem. Soc. 2011, 133, 2772–2782

Scheme 2

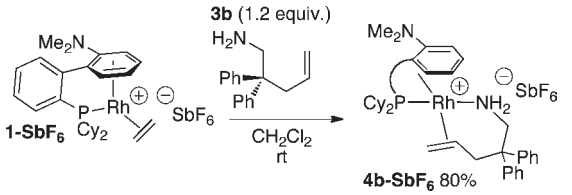

were invariant in the individual solvents, but sharp signals were observed in the NMR spectra of these species, implying that the two stereoisomers equilibrate rapidly on the laboratory time scale, but slowly on the NMR time scale. Binding of the alkene was evidenced by upfield shifts of the olefinic resonances located at 4.3−4.8, 3.37−3.6, and 2.8−2.9 ppm in the complex. ^{103}Rh−^{13}C coupling was observed in all four of the olefinic ^{13}C NMR signals corresponding to the two diastereomeric forms of **4b** (J = 15 and 14 Hz for the resonances at 52 and 55 ppm corresponding to the vinylidene carbons and 15 and 16 Hz for the resonances at 68 and 69 ppm corresponding to the internal alkene carbons of the two diastereomers). The similarity of the chemical shifts and coupling constants for the analogous resonances of the two diastereomers implies that the two isomers result from binding of the metal to the two faces of the alkene, rather than from a cis and trans disposition of the amino or alkene group to the phosphorus atom.

Binding of the amine portion of the primary aminoalkene was deduced from the ^{2}H NMR and ^{31}P NMR chemical shifts and the value of J_{Rh-P}. We used ^{2}H NMR spectroscopy to measure the chemical shift of the amino protons so that they would be clearly distinguished from the many cyclohexyl resonances. The ^{2}H NMR chemical shift of **4b**-d_2 (1.53 ppm) was downfield of that of the free primary aminoalkene **3b**-d_2 (0.71 ppm), indicating that the amine was significantly perturbed by binding of the substrate. In addition, the ^{31}P NMR chemical shifts of the diastereomers of complex **4b** (47.8 and 46.6 ppm) and the J_{Rh-P} values (143 and 142 Hz) were closer to those of the amine complex (56.9 ppm, 159 Hz, vide infra) than to those of complex **1** containing a bound alkene and an η^6 arene ligand (71.7 ppm, 191 Hz). Finally, the reduced hapticity of the arene ligand was indicated by the downfield shift of the arene resonances from the region of η^6-arene complexes observed for complex **1** to the more typical region of aromatic resonances.

Single crystals of **4b-SbF$_6$** were obtained from a mixture of CH_2Cl_2 and pentane, and the structure in the solid state is consistent with that deduced from the solution NMR data. An ORTEP diagram of **4b-SbF$_6$** is shown in Figure 3. This complex clearly adopts a structure with the ligand bound in a κ^1-η^2 form through the C=C bond containing the carbon ipso to the second aryl ring and the unsubstituted ortho carbon. Such a binding mode is distinct from that in which a metal is bound in a κ^1 mode to the arene portion of the ligand at the carbon ipso to the second aryl group.[58] The degree of pyramidalization of the dimethylamino group on the arene in **4b-SbF$_6$** ($\sum_{CNC}$ = 350.2°) is more akin to that in **2** ($\sum_{CNC}$ = 352.6 and 356.7°) than to that in the ethylene complex **1** ($\sum_{CNC}$ = 359.8°). The amino group is bound to rhodium with a Rh−N distance (2.124(7) Å) that is longer than the Rh−N distances to the acetonitrile ligands in **2**. The alkene C=C distance remains that of an electrophilic alkene; the C=C distance of the coordinated alkene (1.375(12) Å) is within experimental error of the C=C distance in ethylene complex **1**,

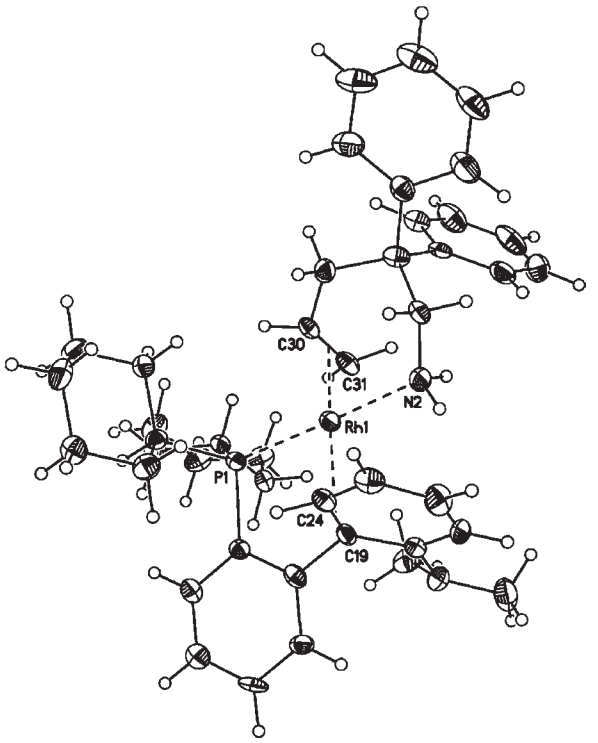

Figure 3. ORTEP diagram of the cationic portion of [Rh(L)(CH$_2$=CHCH$_2$CPh$_2$CH$_2$NH$_2$)]SbF$_6$ (**4b-SbF$_6$**). Ellipsoids are shown at 50% probability. The counterion is omitted for clarity.

and the Rh−C distances of 2.111(7) and 2.144(8) Å straddle those of **1**.

To gather further information on the binding of primary amines to the **L**Rh$^+$ fragment, we prepared and obtained structural data on a complex containing two primary amine donors. The reaction of ethylene complex **1** with ethylenediamine in THF at room temperature generated a complex **5** in which both amino groups are bound to the metal (eq 3). This binding of two dative donors was, again, accompanied by a reduction in the hapticity of the arene portion of the ligand. This reduced hapticity in solution was evidenced by the upfield ^{13}C NMR resonances for the ipso and the unsubstituted ortho carbons (81.3 and 85.3 ppm) and typical aromatic resonances for the other carbons in the bound ring.

The structure deduced by NMR was corroborated by X-ray diffraction (Figure 4). In this structure, the biaryldialkylphosphine ligand clearly bound in an η^2, κ^1 mode with a Rh−P distance (2.2120(9) Å) that is 0.03 Å shorter than that in complex **1**, which contains the η^6-arene, and nearly identical to the distance in acetonitrile-complex **2**, which contains the η^2-arene. The Rh−C$_{ipso}$ distance (2.180(3) Å) is similar to that in **1** (2.166(3) Å) and 0.03 Å longer than that in **2**, but the Rh−C$_{ortho}$ distance (2.191(3) Å) is 0.08 Å shorter than that in **1** (2.271(3) Å) and 0.2 Å longer than that in **2** (2.214(3) and 2.215(3) Å). Again, the dimethylamino group on the arene is more pyramidized ($\sum_{CNC}$ = 350.8°) than that in the ethylene complex **1** ($\sum_{CNC}$ = 359.8°) and similar to that in **2** (352.6 and 356.7°). Finally, like the Rh−N distances to the acetonitrile ligands in **2**, the Rh1−N1 distance (2.145(3) Å) to the nitrogen trans to the phosphine is longer than the Rh1−N2 distance (2.101(3) Å) located trans to the η^2-arene ligand, and the

dx.doi.org/10.1021/ja1057949 |J. Am. Chem. Soc. 2011, 133, 2772–2782

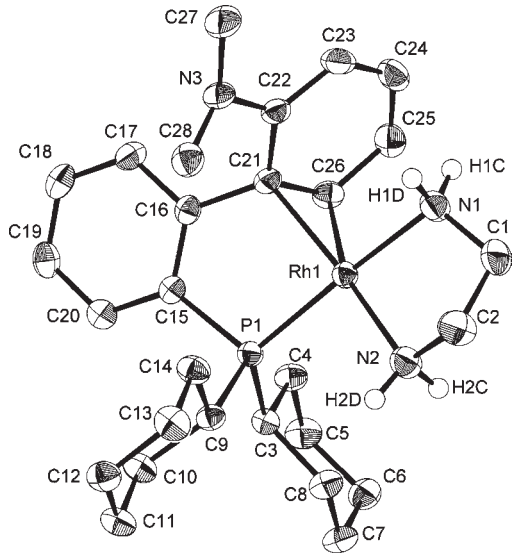

Figure 4. ORTEP diagram of the cationic portion of [Rh(L)(ethylenediamine)]BF_4 (**5**). Ellipsoids are shown at 50% probability. Counterion, solvent, and all hydrogen atoms other than that of amino group are omitted for clarity.

distance trans to phosphorus is longer than that of the amino group in **4b-SbF$_6$** (2.124(7) Å), which is trans to phosphorus.

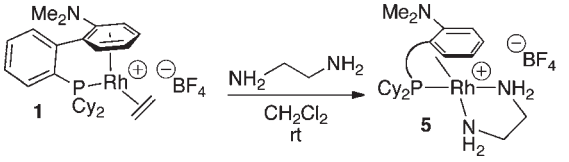

(3)

2.2. Relative Binding Abilities of the Aminoalkenes and the Phosphine. To reveal factors controlling the reactivity of this catalyst system toward primary and secondary amines and to probe pathways for catalyst decomposition, we studied the relative binding affinities of the rhodium for the primary aminoalkene, the secondary aminoalkene, and the phosphine ancillary ligand. These studies showed that binding of the primary aminoalkene was favored over binding of the secondary amine. Treatment of secondary aminoalkene complex **4a** with 1.5 equiv of the primary aminoalkene **3b** led to quantitative formation of the primary aminoalkene complex **4b** (eq 4). In this case, the pseudo square-planar geometry of the primary aminoalkene complex and the bidentate binding mode of the primary aminoalkene within this structure likely account for the exclusive binding of this substrate to the **L**Rh fragment.[59]

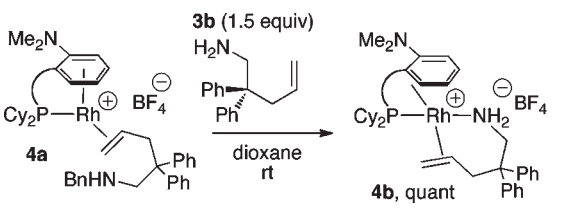

(4)

These studies also showed that the phosphine and the aminoalkene bound competitively to the Rh(COD)$^+$ and Rh(aminoalkene)$^+$ fragments (Scheme 3). The reaction of

Scheme 3

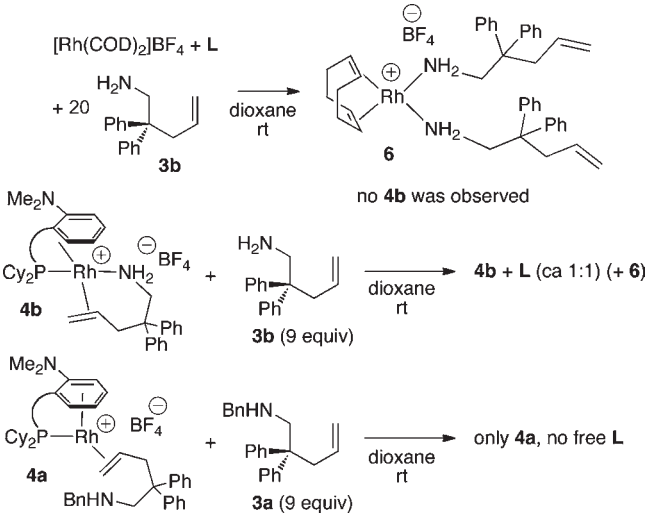

$[Rh(COD)_2]BF_4$ in the presence of 20 equiv of the primary aminoalkene and 1 equiv of the ligand in dioxane led to a solution containing free phosphine ligand and no detectable coordinated phosphine. Instead, the complex [Rh(COD)(1°-aminoalkene)$_2$]BF_4 (**6**) was observed. Consistent with the competitive binding of the aminoalkene and the phosphine, reaction of the primary aminoalkene complex **4b** with an excess (9 equiv) of free aminoalkene **3b** in the same solvent led to a roughly 1:1 ratio of **4b** to free phosphine.[60] In contrast to reaction of the primary aminoalkene complex **4b** with excess of the primary aminoalkene **3b**, reaction of the secondary aminoalkene complex **4a** with an excess of the secondary aminoalkene **3a** in dioxane did not lead to the generation of free phosphine ligand.

The cationic bis-amine complex **6** was isolated and fully characterized and is related to the bis-amine complex [Rh(COD)(morpholine)$_2$]$^+$ reported by Beller.[11] The similarity between the chemical shifts of the olefinic resonances of **6** (4.9−5.3 ppm) and those of the free aminoalkene (5.0−5.46 ppm), along with the lack of Rh−C coupling to the alkene, indicate that the amine nitrogen, not the alkene C=C bond, is bound to rhodium. The connectivity of this species was confirmed by X-ray diffraction, although the quality of the crystal did not allow detailed reporting of metrical parameters.

3. Evaluation of the Competence of the Observed Species to be Intermediates. Ethylene complex **1**, acetonitrile complex **2**, and secondary and primary aminoalkene complexes **4a**,**b** are competent to be intermediates in the cyclization of primary and secondary aminoalkenes **3a**−**c** or to lead to an intermediate by a low-energy process. Secondary aminoalkene complex **4a** reacted in THF at 20 °C within 5 h to form the cyclic hydroamination product **7a** in quantitative yield (eq 5). The rhodium from this process precipitated from solution, and we were not able to characterize it. The reaction of *N*-*p*-chlorobenzylaminoalkene **3c** catalyzed by 2.5 mol % of **4a** with 5 mol % added COD (to help stabilize the catalyst, vide infra) in dioxane-d_8 at 70 °C gave **7c** in 98% yield after 26 h (eq 6).

Primary aminoalkene complex **4b** also underwent cyclization. This complex reacted in dioxane at 100 °C within 5 min to form the cyclic amine **7b** in 53% yield (eq 7). This reaction conducted with addition of a different primary aminoalkene occurred in a higher

dx.doi.org/10.1021/ja1057949 |*J. Am. Chem. Soc.* 2011, 133, 2772–2782

80% yield.[61] Reaction of primary aminoalkene **3b** catalyzed by 5 mol % of **4b** with 10 mol % added COD in dioxane at 100 °C gave **7b** in 82% yield after 3 h (eq 8). The yield of this reaction was somewhat higher in the absence of added COD and similar in the presence of added **L**.

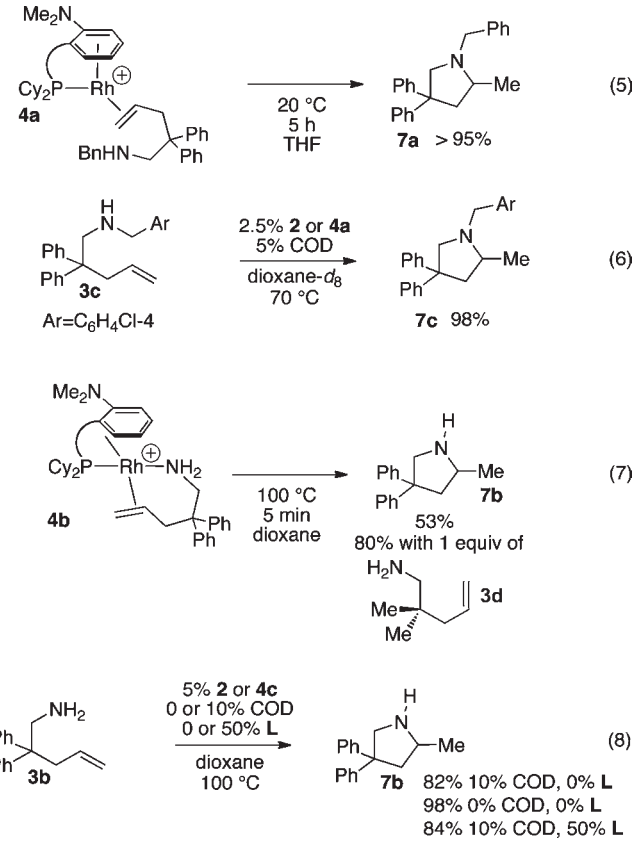

Side-by-side reactions of secondary aminoalkene **3a** catalyzed by the combination of $[Rh(COD)_2]BF_4$ and **L**, by isolated acetonitrile complex **2**, and by isolated aminoalkene complex **4a** showed that the reactions catalyzed by the preformed η^6, κ^1 species are faster than those catalyzed by the original system. The half-life of the latter two reactions was about 8 h, whereas only 10% conversion to product was observed after this time from the reaction of **3a** catalyzed by $[Rh(COD)_2]BF_4$ and **L**.

4. Identification of the Catalyst Resting State. To determine the resting state of the catalyst, we monitored by ^{31}P NMR spectroscopy reactions of the secondary and primary aminoalkene complexes catalyzed by several catalyst precursors and aminoalkene complexes. Monitoring the reactions of the secondary aminoalkene **3a** catalyzed by 2.5 mol % $[Rh(COD)_2]BF_4$ and 3 mol % **L** or by 2.5 mol % acetonitrile complex **2** in dioxane showed that the secondary aminoalkene complex **4a** was the only rhodium−phosphine complex observed throughout either reaction. Some catalyst decomposition over the course of this reaction was observed; the rhodium catalyst was lost from the system over time as a black precipitate and some free **L** accumulated. The addition of COD helped preserve the active catalyst, and, therefore, some of the kinetic studies (vide infra) were conducted with added COD.

Reactions of primary aminoalkene **3b** catalyzed by 5 mol % of acetontrile complex **2** or 5 mol % of $Rh(COD)_2BF_4$ and 6 mol % **L** in dioxane were also monitored by ^{31}P NMR spectroscopy. In reactions catalyzed by **2**, only the signal of primary aminoalkene-complex **4b** was observed before heating, and the signal of **4b** remained the major species observed, along with a small amount of free **L**, after heating for 5 min at 100 °C. As the catalytic reaction progressed, the signal of **4b** decayed, and the signal due to free **L** increased. After 10 min at 100 °C, about 30% of the ligand had dissociated. At the end of the reaction, new four doublet signals and the signal of free **L** was observed. In the reactions catalyzed by the combination of $Rh(COD)_2BF_4$ and **L**, the red color of complex **4b** was not observed at room temperature. Instead, the yellow bis-amine complex **6** was likely generated, as suggested by the yellow color of the solution. Heating of this mixture at 100 °C generated a small amount of **4b**, but free **L** was the major species observed by ^{31}P NMR spectroscopy, and the ratio of **4b** to **L** was approximately 1:20. Thus, binding of the aminoalkene over the phosphine limits the reactivity of this catalyst for cyclization of aminoalkenes.

5. Reactions of Deuterated Amines. 5.1. Probes for Direct versus Indirect Addition Pathways. The cyclic amine could form by direct addition of the N−H bond to the alkene, or it could occur by oxidative amination, followed by addition of the released hydrogen to the resulting enamine. To distinguish between these mechanisms, we conducted the reaction of the deuterated *N*-*p*-chlorobenzylamine **3c**-*N*-d_1 shown in eq 9.

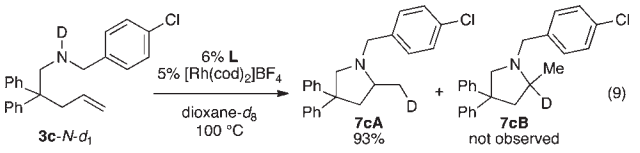

Oxidative amination, followed by addition of the released equivalent of H−D, would form the two isotopomers **7cA** and **7cB** in eq 9. However, direct addition would form the single isotopomer **7cA**. Consistent with direct addition, **3c**-*N*-d_1 reacted in the presence of 5 mol % of $[Rh(COD)_2]BF_4$ and 6% of **L** to form **7cA** in 93% yield, with 93% deuterium content and without formation of **7cB**.

5.2. Stereochemistry of the Hydroamination Process. Several catalytic cycles can be envisioned for the observed hydroamination process starting from substrate complexes **4a** and **4b** (Scheme 4). Complex **4a** containing the secondary amine could react by the combination of external attack of the amine on the coordinated alkene and protonolysis of the resulting Rh−C bond (path A). Complex **4b** containing the primary amine could react by an analogous path after dissociation of the amino group. Complex **4a** could react by the combination of olefin dissociation, N−H bond activation, and olefin insertion into the amide or hydride ligand, and complex **4b** could react by N−H bond activation and analogous olefin insertion (path B). Finally, these complexes could react by the generation of an amido complex, perhaps by deprotonation of the substrate bound to the metal through the amino group, followed by insertion of the alkene to form an aminoalkyl complex that undergoes protonolysis to release the amine product (path C).

To distinguish mechanisms involving nucleophilic attack on an alkene from those involving migratory insertion of the alkene, we determined the stereoisomer formed by hydroamination of a 1,2-disubstituted alkene. Reaction by nucleophilic attack, followed by protonolysis, would yield the product of anti addition across the alkene. Reaction by a pathway involving insertion, followed by reductive elimination or protonolysis, would yield the product of syn addition across the alkene.

dx.doi.org/10.1021/ja1057949 |*J. Am. Chem. Soc.* 2011, 133, 2772–2782

Scheme 4

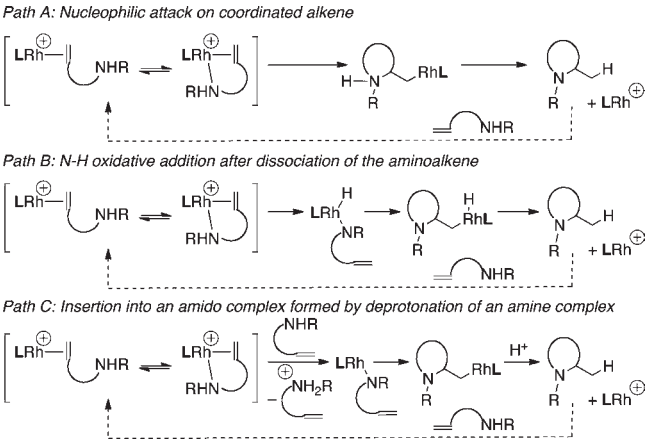

If the stereochemistry of this process is to be evaluated, the catalyst must lead to addition across an internal alkene. To generate a substrate for such an addition, we prepared aminoalkenes **8a**-*N*-d_1 and **8b**-*N*-d_2 in eq 10. Reaction of aminoalkene **8a**-*N*-d_1 in the presence of 5 mol % $[Rh(COD)_2]BF_4$ and 6 mol % **L** led to the cyclization product **9a**-*d*, and reaction of aminoalkene **8b**-*N*-d_2 in the presence of this catalyst led to the cyclization product **9b**-*d*. Although the reaction of **8a**-*N*-d_1 occurred in modest yield,[62] a sufficient amount of pure product was isolated to obtain spectral data to analyze the stereochemical outcome of the addition. The reaction of **8b**-*d* occurred in higher yield. The N−D of **9b**-*d* exchanged upon workup, but deuterium incorporation at the new position β to the amino group in both products was about 75%.

The relative stereochemistry in the product was assessed by a combination of ^{1}H-COSY and 1D-NOE spectroscopy. Details of this analysis are provided as Supporting Information. In brief, an NOE was observed between H^a and H^d in the products of eq 10, indicating a 1,3-cis diaxial relationship between these two hydrogens, and an NOE was observed between H^a and H^b, indicating a cis 1,2-relationship. The resonance corresponding to H^d located trans to the amino nitrogen is the one at the chemical shift in the ^{2}H NMR spectrum of the product **9**-*d* formed from reaction of **8**-*N*-d_1. Thus, the amino group in the product is trans to the deuterium, and the addition of the N−H bond across the alkene occurs in an anti fashion.

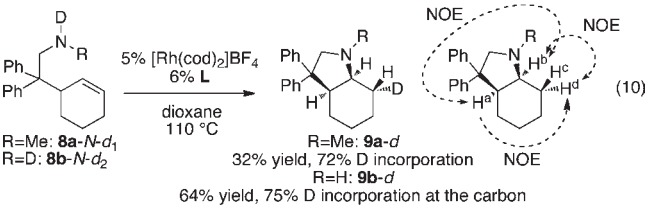

6. Evaluation of the Stereochemistry of Additions of H_2 and Silanes Catalyzed by Acetonitrile Complex 2. As noted in the Introduction, most rhodium-catalyzed reactions of X−H bonds across alkenes lead to products of syn addition, while complexes of many other metals catalyze reactions of N−H bonds across alkenes to form products of anti addition. To determine if the relative configuration in the product of our rhodium-catalyzed hydroamination results from the unusual structure of the metal−ligand complex or the unusual reaction of an N−H bond by a rhodium system, we determined the stereochemical outcome of the addition of D_2 and $DSiEt_3$ to norbornene catalyzed by **2**. When examined, rhodium-catalyzed hydrogenations and hydrosilylations occur by syn addition to alkenes.

Scheme 5

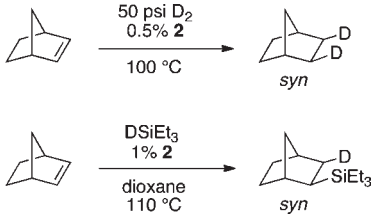

Scheme 6

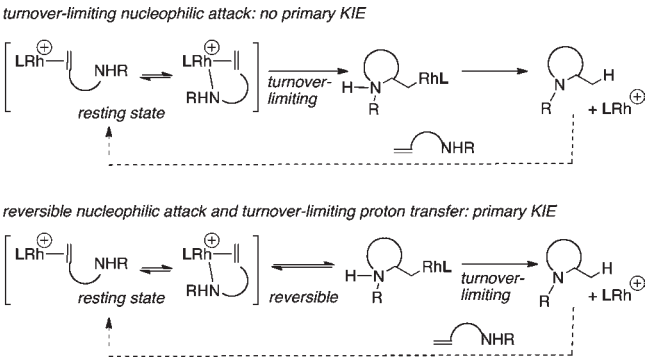

The reaction of norbornene with 50 psi D_2 at 100 °C or $DSiEt_3$ at 110 °C catalyzed by acetonitrile complex **2** gave the stereoiosomers of norbornane-d_2 and *exo*-2-deuterio-*exo*-3-triethylsilylnorbornane that reflect a cis addition (Scheme 5). Thus, the trans addition pathway results from the amine reagent, not from the particular coordination sphere of the rhodium catalyst.

7. Kinetics of the Addition Process. To identify the turnover-limiting step of the catalytic process and any reversible processes that would precede this step, we conducted kinetic studies on the cyclization process. Complexes **4a** and **4b** containing acyclic secondary aminoalkene bound through the alkene (**4a**) and the acyclic primary aminoalkene bound through the olefin and amino group (**4b**) were the observed resting states when reactions were initiated with acetonitrile complex **2** or the aminoalkene complexes as catalyst, at least at early reaction times before substantial competitive decomposition of the catalyst occurred (vide supra). Two mechanisms leading to the trans addition products could operate with complexes **4a** and **4b** as the resting state (Scheme 6). First, the reaction could occur by turnover-limiting attack of the amino group on the coordinated alkene directly within the olefin-bound aminoalkene complex **4a** or after dissociation of the amino group in complex **4b** in which the amino and olefin groups are both bound to rhodium. Alternatively, an initial, thermodynamically unfavorable, reversible attack of the amine on the alkene, followed by turnover-limiting proton transfer to release the aminoalkene, could lead to the product and would occur with the observed resting states. These two scenarios can be distinguished by the kinetic isotope effect. A primary isotope effect would not be observed if

dx.doi.org/10.1021/ja1057949 |J. Am. Chem. Soc. 2011, 133, 2772–2782

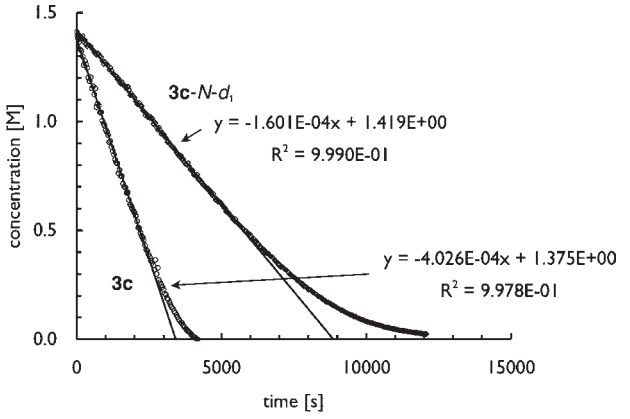

Figure 5. Profiles for the decay of secondary aminoalkenes **3c** and **3c**-*N*-d_1 in the presence of 1.25 mol % [Rh(L)(NCMe)$_2$] (**2**) and 10 mol % COD at 100 °C in dioxane-d_8. The linear fit to the decay of **3c** corresponds to a fit to the first 67 data points (2600 s); the linear fit to the decay of **3c**-*N*-d_1 corresponds to a fit to the first 150 data points (6000 s).

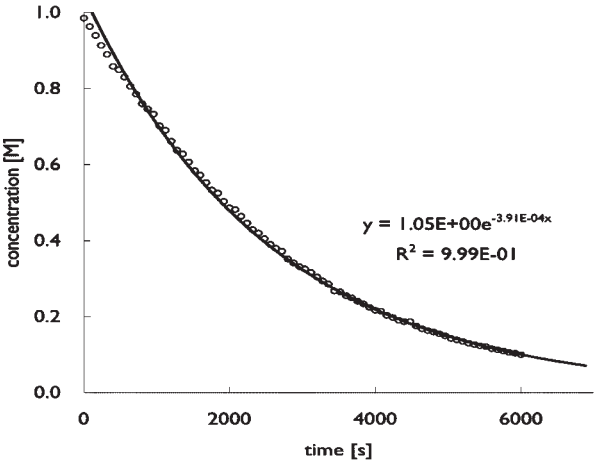

Figure 6. Profiles for the decay of secondary aminoalkene **3c** in the presence of 1.25% [Rh(L)(NCMe)$_2$]BF$_4$ (**2**) and 1 equiv (vs **3c**) of COD at 100 °C in dioxane-d_8. The curve corresponds to an exponential decay of **2** with a rate constant of 3.9×10^{-4} s^{-1}.

nucleophilic attack were turnover limiting, but a primary isotope effect would be observed if nucleophilic attack were reversible and followed by turnover-limiting proton transfer.

The profiles for cyclization of **3c** and **3c**-*N*-d_1 catalyzed by **2** in the presence of a small amount of COD to stabilize the catalyst (vide supra) are shown in Figure 5. These decays indicate that the reaction is zero-order in **3c** when the concentration of **3c** is much larger than that of the added COD. When the substrate concentration is high, the added COD does not compete with **3c** for the open coordination site. Under these conditions, k_H/k_D is 2.5 ± 0.6. This clear primary isotope effect contrasts with that of the cyclization of primary aminoalkenes by a rhodium catalyst containing the aminophosphine derivative of Xantphos.[28] Consistent with competitive binding of COD and the aminoalkene, the reaction was first-order in the aminoalkene **3c** when the reaction was run with 1 equiv of COD (Figure 6).

The zero-order rate behavior with a small amount of added COD, primary isotope effect, and the presence of **4a** as the resting state imply that the turnover-limiting step involves proton transfer in a transition state comprised solely of the components contained within **4a**. These data are consistent with the mechanism involving reversible nucleophilic attack of the amine on the alkene, followed by turnover-limiting intramolecular protonation of the Rh−C bond, as shown in the bottom scenario in Scheme 6.

The kinetic behavior of the reactions of primary amines was more complex due to equilibria involving competitive binding of the amine and the phosphine and the shorter lifetime of the catalyst. Thus, reactions of the primary amine catalyzed by acetonitrile complex **2** occurred with neither simple first nor simple zero-order decay profiles. ^{31}P NMR spectra indicated that a significant amount of free phosphine was contained in this system. Thus, some rhodium of the rhodium in the system lacks coordinated phosphine.

This observation suggested that the rates of the hydroamination would be positive order in added phosphine. If the active catalyst contains the phosphine, and if the rhodium lacking phosphine and rhodium bound by phosphine are in equilibrium, then the reaction would occur with a positive order in this added ligand, as summarized in Scheme 7. Moreover, if the active catalyst contains the phosphine and the equilibrium between the bound and free species lies further toward the bound species at higher concentrations of

Scheme 7

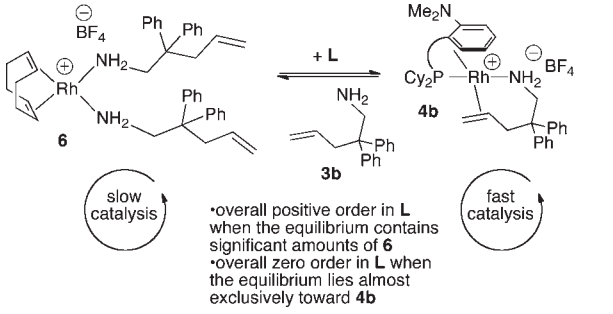

added ligand, then the order in ligand should decrease as the population of rhodium is shifted toward the active ligated species. If the rhodium were fully bound by phosphine and remained in this state throughout the catalytic cycle (or if the barrier for exchange between free and bound rhodium is high enough that these species are not in equilibrium), then the reaction would be zero-order in phosphine. If reversible ligand dissociation occurs prior to the turnover-limiting step or the active catalyst lacks the phosphine ligand (Scheme 7), then the reaction would occur with an inverse order in phosphine.

The profiles for cyclization of primary aminoalkenes **3b** and **3b**-*N*,*N*-d_2 catalyzed by **2** in the absence of COD are shown in Figure 7. From initial rates, the value of k_H/k_D was found to be ca. 2.4 ± 0.2. At the end of the reaction, rhodium black was not observed, and four unidentified doublet signals and free L were observed by ^{31}P NMR spectroscopy.

A second set of experiments was run in the presence of 10 mol % added COD, which is present in the catalyst precursor and was present in our preparative reactions of secondary aminoalkenes initiated with isolated acetonitrile complex **2**.[27] The added COD appeared to stabilize the catalyst, but to retard the cyclization. We measured the reaction rates as a function of the concentration of ligand and obtained several pieces of data that argue for reaction through the observed amine complex ligated by the phosphine in equilibrium with an inactive phosphine-free complex. First, as

dx.doi.org/10.1021/ja1057949 |*J. Am. Chem. Soc.* 2011, 133, 2772–2782

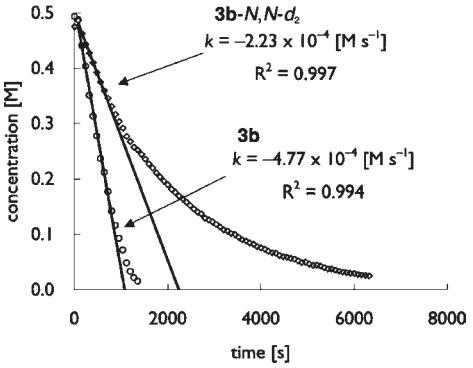

Figure 7. Profiles for the decay of primary aminoalkenes **3b** and **3b**-*N*,*N*-d_2 in the presence of [Rh(L)(NCMe)$_2$] (**2**) at 100 °C in dioxane-d_8 with no added COD. From a least-squares fit for initial rates using the first eight data points, k_H/k_D = 2.4 ± 0.2.

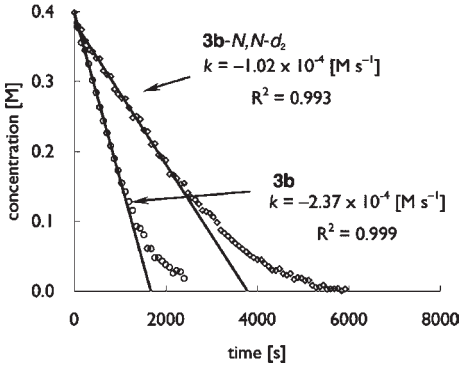

Figure 8. Profiles for the decay of primary aminoalkene **3b** in the presence of 5% [Rh(L)(NCMe)$_2$]BF$_4$ (**2**), 18% **L**, and 10% COD at 100 °C in dioxane-d_8. From a least-squares fit to the data over the first 50% conversion, k_H/k_D = 2.3 ± 0.2.

shown in Figure 8, reactions catalyzed by **2** with 18 mol % added ligand occurred with a profile that was consistent with a zero-order reaction. This reaction profile was analogous to that in Figure 5 for the reaction of the secondary aminoalkene **3c**. Under these conditions, k_H/k_D was found to be 2.3 ± 0.2. This value is indistinguishable from the value obtained in the absence of added COD. Second, a plot of k_{obs} versus [**L**] (Figure 9) had a clear positive slope, indicating that the reaction occurs with a positive dependence on free ligand. We hesitate to fit these data to a precise equation because the catalyst lifetime is short at the lower [**L**], but this plot is qualitatively consistent with an equilibrium in the catalytic system between a phosphine-free rhodium that is catalytically inactive and phosphine-bound rhodium that is catalytically active. Consistent with this assertion, the reaction of primary aminoalkene **3b** catalyzed by 5 mol % phosphine-free bis-amine complex [(COD)Rh(aminoalkene)$_2$]$^+$ (aminoalkene = **3b**) **6** in dioxane-d_8 was slow, and after 24 h gave about 10% of an aminoalkene containing an internal olefin from isomerization, 15% imine, and only 5% cyclized product (eq 11).

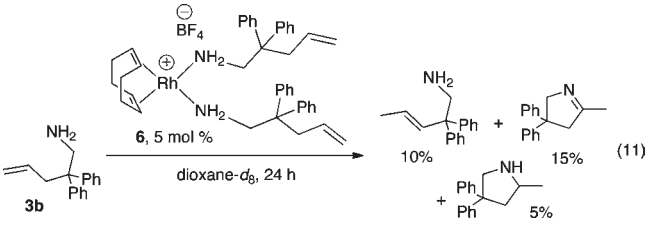

(11)

8. Independent Synthesis of an LRh−Alkyl Complex and Evaluation of the Rate of Protonolysis. If the hydroamination process occurs by nucleophilic attack of the amine on the alkene, followed by protonolysis, then an alkylrhodium complex containing the η^6, κ^1-bound ligand **L** must undergo protonolysis with a rate that is equal to or greater than that of the catalytic process. If nucleophilic attack is a thermodynamically unfavorable and reversible step that occurs prior to protonolysis, then this protonolysis process must be faster than the catalytic reaction. Many alkyl complexes of the late transition metals are kinetically stable to mild acids. Thus, it was not clear a priori whether an alkylrhodium complex of ligand **L** would undergo fast proton transfer.

To assess the rate of protonation of the proposed alkylrhodium intermediate, we conducted the reaction of an ammonium

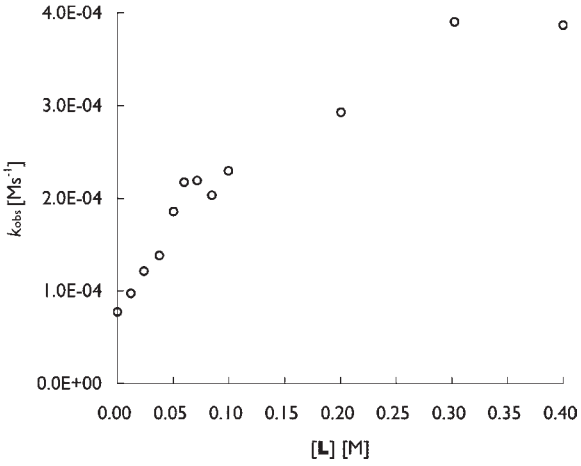

Figure 9. Plot of k_{obs} versus [**L**] for the reaction of primary aminoalkene **3b** in the presence of 5% [Rh(L)(NCMe)$_2$]BF$_4$ (**2**), 0−100% **L**, and 10% COD at 100 °C in dioxane-d_8.

salt with an alkyl complex containing the η^6, κ^1-bound ligand **L**. We did not find a means to conduct this reaction on a β-aminoalkyl species without elimination of the amino group. Thus, we prepared instead an alkylrhodium complex lacking β-hydrogens and containing ligand **L**.

Neopentylrhodium complex **11** was prepared by the addition of neopentylmagnesium chloride to the rhodium chloride complex **10** at room temperature, as shown in eq 12. This species was unstable at room temperature and was, therefore, characterized in solution (see the Supporting Information for data). The presence of a rhodium-bound neopentyl group was revealed by the coupling of the neopentyl methylene carbon and hydrogens to the ^{103}Rh nucleus, and the π-bound arene ring was identified by the presence of resonances upfield of the typical aromatic region.

The reaction of tri-*n*-butylammonium chloride with **11** formed the chloride complex **10** (82%) and neopentane (quantitative yield) at room temperature in only 10 min. The rate of this process is much faster than the catalytic reaction that requires hours at elevated temperatures. This result implies that the proposed protonolysis of the alkylrhodium

dx.doi.org/10.1021/ja1057949 |J. Am. Chem. Soc. 2011, 133, 2772–2782

Scheme 8

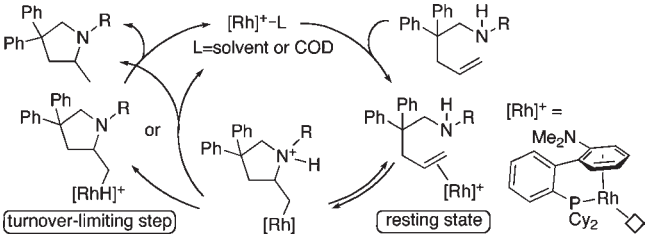

intermediate containing a pendant ammonium acid is sufficiently fast to be part of the catalytic cycle.

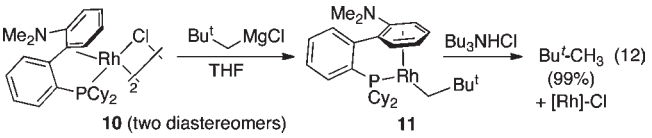

9. Overall Mechanism of the Hydroamination Process. The identification of η^6,κ^1 biaryldialkylphosphine complexes as the active catalyst, olefin complex **4a** and amine complex **4b** as the resting states, trans stereochemistry for addition to the alkene, and primary kinetic isotope effect altogether point to the mechanism shown in Scheme 8. In this scheme, the aminoalkene displaces solvent or residual COD ligand to form an alkene complex when the substrate contains a secondary amine or to form an amine complex when the substrate contains a primary aminoalkene. This binding is then followed by reversible attack of the amino group on the bound alkene. Such nucleophilic attack on a bound alkene is not common for rhodium systems,[49,63] but is a common reaction for cationic olefin complexes of other late transition-metal systems.[64,65] Cyclization of primary amines has been more challenging to develop with late transition-metal catalysts than cyclization of secondary amines,[13,14,28] and this study illustrates explicitly that the greater binding affinity of the primary amine is the likely origin of this trend.

The aminoalkyl intermediate resulting from this nucleophilic attack then undergoes protonolysis. This protonolysis appears to be an intramolecular process[66,38] because the reaction occurs with zero-order kinetics from the resting state containing the bound substrate. This observation precludes the participating of a second metal or second substrate prior to or during the turnover-limiting step. This protonolysis process can occur by direct transfer of the proton to the metal, followed by reductive elimination to form a C−H bond or by proton transfer directly to the Rh−C bond. Recent computational studies of the protonolysis of an iridium ammoniumalkyl complex implied that protonolysis of the metal was favored,[15] but direct protonolysis of the metal−C bond could be favored for the rhodium complex because of the lower basicity of second row metals versus third-row metals. In either case, the overall pathway in Scheme 8, particularly the anti addition, is more closely related to that of palladium- and platinum-catalyzed hydroamination reactions than that of rhodium-catalyzed additions of H_2, H−Si, H−B, and H−C bonds across alkenes.

10. Proposed Origins of the Selectivity for Hydroamination over Oxidative Amination. Our identification of the elementary steps of the catalytic cycle and the precise species undergoing these steps allows us to make an experimentally grounded proposal about why this system leads to products from hydroamination when other rhodium catalysts have led to predominant[11,67] or substantial[12] amounts of products from oxidative amination. With a η^6,κ^1-bound ligand on Rh(I), attack of the amine on the coordinated alkene generates a coordinatively saturated, 18-electron aminoalkyl complex. Such a coordination sphere disfavors β-hydrogen elimination due to the lack of an open coordination site.[68−70] This lack of an open coordination site appears to make this aminoalkyl complex sufficiently stable that the rate of proton transfer to form amine exceeds that of β-hydrogen elimination.

The use of these data to design more active and stable catalysts based on the π,σ-binding mode of the ligand in this catalyst is in progress, and two weak points must be addressed to improve upon the existing system. First, the alkene complex containing the η^6,κ^1-bound **L** contains a significant degree of strain. The bond angles in the structure and the alternative η^2,κ^1-binding mode of several species reveal this strain, and the precipitation of a rhodium species during the reaction suggests that this strain limits the stability of the metal−ligand complex at elevated temperatures in the presence of high concentrations of amine and alkene donors. Second, the rate is limited by the combination of nucleophilic attack by the amine and proton transfer. One would expect that these two steps are favored by opposite changes to the electronic properties of the metal. Thus, an analysis of the sensitivity of these steps to changes in the ancillary ligand is needed to design a system in which the combination of these two steps is faster than it is with the current system. Studies to address these various issues will be the subject of future studies.

■ ASSOCIATED CONTENT

Supporting Information. Experimental procedures, compound characterization, and kinetic plots. This material is available free of charge via the Internet at http://pubs.acs.org.

■ AUTHOR INFORMATION

Corresponding Author
jhartwig@illinois.edu

■ ACKNOWLEDGMENT

We thank the NIH for support (R37-GM055382) and Johnson-Matthey for a gift of $RhCl_3$.

■ REFERENCES

(1) Hartwig, J. F. *Pure Appl. Chem.* **1999**, *71*, 1417.
(2) Muller, T. E.; Hultzsch, K. C.; Yus, M.; Foubelo, F.; Tada, M. *Chem. Rev.* **2008**, *108*, 3795.
(3) Hong, S.; Marks, T. J. *Acc. Chem. Res.* **2004**, *37*, 673.
(4) Müller, T. E. In *Encyclopedia of Catalysis*; Horváth, I. T., Ed.; Wiley-Interscience: Hoboken, 2003; Vol. 3, p 518.
(5) Casalnuovo, A. L.; Calabrese, J. C.; Milstein, D. *J. Am. Chem. Soc.* **1988**, *110*, 6738.
(6) Dorta, R.; Egli, P.; Zurcher, F.; Togni, A. *J. Am. Chem. Soc.* **1997**, *119*, 10857.
(7) Seligson, A. L.; Trogler, W. C. *Organometallics* **1993**, *12*, 744.
(8) Kawatsura, M.; Hartwig, J. F. *Organometallics* **2001**, *20*, 1960.
(9) Kawatsura, M.; Hartwig, J. F. *J. Am. Chem. Soc.* **2000**, *122*, 9546.
(10) Utsunomiya, M.; Hartwig, J. F. *J. Am. Chem. Soc.* **2003**, *125*, 14286.
(11) Beller, M.; Trauthwein, H.; Eichberger, M.; Breindl, C.; Herwig, J.; Muller, T. E.; Thiel, O. R. *Chem.-Eur. J.* **1999**, *5*, 1306.
(12) Utsunomiya, M.; Kuwano, R.; Kawatsura, M.; Hartwig, J. F. *J. Am. Chem. Soc.* **2003**, *125*, 5608.

(13) Bender, C. F.; Widenhoefer, R. A. *J. Am. Chem. Soc.* **2005**, *127*, 1070.
(14) Hesp, K. D.; Stradiotto, M. *Org. Lett.* **2009**, *11*, 1449.
(15) Hesp, K. D.; Tobisch, S.; Stradiotto, M. *J. Am. Chem. Soc.* **2010**, *132*, 413.
(16) LaLonde, R. L.; Sherry, B. D.; Kang, E. J.; Toste, F. D. *J. Am. Chem. Soc.* **2007**, *129*, 2452.
(17) Kimura, M.; Tanaka, S.; Tamaru, Y. *Bull. Chem. Soc. Jpn.* **1995**, *68*, 1689.
(18) Liu, G. S.; Lu, X. Y. *Org. Lett.* **2001**, *3*, 3879.
(19) Zhang, Z.; Liu, C.; Kinder, R. E.; Han, X.; Qian, H.; Widenhoefer, R. A. *J. Am. Chem. Soc.* **2006**, *128*, 9066.
(20) Zhang, Z.; Bender, C. F.; Widenhoefer, R. A. *J. Am. Chem. Soc.* **2007**, *129*, 14148.
(21) Kinder, R. E.; Zhang, Z.; Widenhoefer, R. A. *Org. Lett.* **2008**, *10*, 3157.
(22) Giner, X.; Najera, C. *Org. Lett.* **2008**, *10*, 2919.
(23) Bender, C. F.; Widenhoefer, R. A. *Chem. Commun.* **2006**, 4143.
(24) Zhang, J. L.; Yang, C. G.; He, C. *J. Am. Chem. Soc.* **2006**, *128*, 1798.
(25) Liu, X. Y.; Li, C. H.; Che, C. M. *Org. Lett.* **2006**, *8*, 2707.
(26) Michael, F. E.; Cochran, B. M. *J. Am. Chem. Soc.* **2006**, *128*, 4246.
(27) Liu, Z.; Hartwig, J. F. *J. Am. Chem. Soc.* **2008**, *130*, 1570.
(28) Julian, L. D.; Hartwig, J. F. *J. Am. Chem. Soc.* **2010**, *132*, 13813.
(29) Shen, X.; Buchwald, S. L. *Angew. Chem., Int. Ed.* **2010**, *49*, 564.
(30) For a recent example of a system that adds both primary and secondary amines, see ref 15.
(31) Gagné, M. R.; Stern, C. L.; Marks, T. J. *J. Am. Chem. Soc.* **1992**, *114*, 275.
(32) Stubbert, B. D.; Marks, T. J. *J. Am. Chem. Soc.* **2007**, *129*, 6149.
(33) Gribkov, D. V.; Hultzsch, K. C. *Angew. Chem., Int. Ed.* **2004**, *43*, 5542.
(34) Knight, P. D.; Munslow, I.; O'Shaughnessy, P. N.; Scott, P. *Chem. Commun.* **2004**, 894.
(35) Müller, C.; Saak, W.; Doye, S. *Eur. J. Org. Chem.* **2008**, 2731.
(36) Leitch, D. C.; Payne, P. R.; Dunbar, C. R.; Schafer, L. L. *J. Am. Chem. Soc.* **2009**, *131*, 18246.
(37) For a recent study providing evidence for alkene insertion during a hydrohydrazination proess, see: Hoover, J. M.; DiPasquale, A.; Mayer, J. M.; Michael, F. E. *J. Am. Chem. Soc.* **2010**, *132*, 5043.
(38) Cochran, B. M.; Michael, F. E. *J. Am. Chem. Soc.* **2008**, *130*, 2786.
(39) Walsh, P. J.; Baranger, A. M.; Bergman, R. G. *J. Am. Chem. Soc.* **1992**, *114*, 1708.
(40) Baranger, A. M.; Walsh, P. J.; Bergman, R. G. *J. Am. Chem. Soc.* **1993**, *115*, 2753.
(41) Wood, M. C.; Leitch, D. C.; Yeung, C. S.; Kozak, J. A.; Schafer, L. L. *Angew. Chem., Int. Ed.* **2007**, *46*, 354.
(42) Gott, A. L.; Clarke, A. J.; Clarkson, G. J.; Scott, P. *Chem. Commun.* **2008**, 1422.
(43) Hartwig, J. F. *Organotransition Metal Chemistry*; University Science Books: Sausalito, CA, 2009; Chapter 16: Hydrofunctionalization and Oxidative Functionalization of Olefins.
(44) *Modern Rhodium-Catalyzed Organic Reactions*; Evans, P. A., Ed.; Wiley-VCH: Weinheim, 2005.
(45) Crabtree, R. H. *The Organometallic Chemistry of the Transition Metals*, 4th ed.; Wiley: New York, 2005; Chapter 9, p 560.
(46) Han, X.; Widenhoefer, R. A. *Angew. Chem., Int. Ed.* **2006**, *45*, 1747.
(47) Kennedy-Smith, J. J.; Staben, S. T.; Toste, F. D. *J. Am. Chem. Soc.* **2004**, *126*, 4526.
(48) For an example in which the reaction of a rhodium−olefin complex led to displacement of the alkene, rather than addition, see ref 49.
(49) Hahn, C.; Sieler, J.; Taube, R. *Chem. Ber.* **1997**, *130*, 939.
(50) Old, D. W.; Wolfe, J. P.; Buchwald, S. L. *J. Am. Chem. Soc.* **1998**, *120*, 9722.
(51) Faller, J. W.; D'Alliessi, D. G. *Organometallics* **2003**, *22*, 2749.
(52) Werner, H.; Canepa, G.; Ilg, K.; Wolf, J. *Organometallics* **2000**, *19*, 4756.
(53) Love, R. A.; Koetzle, T. F.; Williams, G. J. B.; Andrews, L. C.; Bau, R. *Inorg. Chem.* **1975**, *14*, 2653.
(54) Cheng, P. T.; Nyburg, S. C. *Can. J. Chem.* **1972**, *50*, 912.
(55) Rettig, M. F.; Wing, R. M.; Wiger *J. Am. Chem. Soc.* **1981**, *103*, 2980.
(56) Malinoski, J. M.; White, P. S.; Brookhart, M. *Organometallics* **2003**, *22*, 621.
(57) *Tables of Interatomic Distances and Configuration in Molecules and Ions*; Sutton, L. E., Ed.; The Chemical Society: London, 1958.
(58) Christmann, U.; Pantazis, D. A.; Benet-Buchholz, J.; McGrady, J. E.; Maseras, F.; Vilar, R. n. *J. Am. Chem. Soc.* **2006**, *128*, 6376.
(59) For a brief analysis of the strictly κ^1 binding of primary and secondary aminoalkenes to the rhodium catalyst containing an aminophosphine derivative of Xantphos, see ref 28. In this case, the primary amine binds 50−100 times stronger than the secondary aminoalkene, which adopts both N-bound and alkene-bound forms.
(60) A species of unknown structure was detected in the ^{31}P NMR spectrum during this displacement of ligand, perhaps corresponding to a complex with the phosphine bound without an interaction of the rhodium with the arene.
(61) It is possible that the second amine increases the rate of dissociation of a portion of the κ^2-bound aminoalkene or that it binds the rhodium product and prevents decomposition of the reactant by the initial unsaturated rhodium product, but we did not conduct detailed studies on this effect.
(62) We did not seek to optimize the yield of this process.
(63) Hauger, B. E.; Huffman, J. C.; Caulton, K. G. *Organometallics* **1996**, *15*, 1856.
(64) Hartwig, J. F. *Organotransition Metal Chemistry*; University Science Books: Sausalito, CA, 2010; Chapter 11: Nucleophilic Attack on Coordinated Ligands.
(65) Crabtree, R. H. *The Organometallic Chemistry of the Transition Metals*, 4th ed.; Wiley: New York, 2005; Chapter 8, p 560.
(66) For an example of protonolysis of a cationic alkylpalladium species containing nitrogen in the β position, see ref 38.
(67) Beller, M.; Eichberger, M.; Trauthwein, H. *Angew. Chem., Int. Ed. Engl.* **1997**, *36*, 2225.
(68) McCarthy, T. J.; Nuzzo, R. G.; Whitesides, G. M. *J. Am. Chem. Soc.* **1981**, *103*, 3396.
(69) Cross, R. J. In *The Chemistry of the Metal−Carbon Bond*; Hartley, F. R., Patai, S., Eds.; John Wiley: New York, 1985; Vol. 2, p 559.
(70) Hartwig, J. F. *Organotransition Metal Chemistry*; University Science Books: Sausalito, CA, 2010; Chapter 10: Elimination Reactions.